Chemical Physics Letters 720 (2019) 15–18

Contents lists available at ScienceDirect

Chemical Physics Letters

journal homepage: www.elsevier.com/locate/cplett

Research paper

Electronic and transport properties of deformed platinum nanotubes calculated using relativistic linear augmented cylindrical wave method

P.N. D'yachkov[a,*], D.O. Krasnov[a,b]

[a] Kurnakov Institute of General and Inorganic Chemistry, Russian Academy of Sciences, Leninskii Prospekt 31, Moscow 119991, Russia
[b] Dmitry Mendeleev University of Chemical Technology of Russia, Miusskaya sq. 9, Moscow 125047, Russia

HIGHLIGHTS

- The spin- and deformation-dependent band structures of Pt nanotubes are studied.
- The spin-orbit coupling results in a splitting of dispersion curves equal up to 0.5 eV.
- The Pt nanotubes are semimetallic.
- Deformation of tubules can induce a formation of minigaps in a terahertz region.

ARTICLE INFO

Keywords:
Modeling
Platinum
Nanotubes
Quantum chemistry
Spin–orbit coupling
Band structure

ABSTRACT

The spin- and deformation-dependent electron structures of the single-walled chiral and achiral Pt nanotubes are investigated using a relativistic linear augmented cylindrical wave method. It is shown that the Fermi level separates the valence and conduction band curves. The nanotubes are semimetallic. The spin-orbit coupling results in a splitting of dispersion curves equal up to 0.5 eV. The torsional, uniaxial, and uniform strain results in a drastic change of the electronic states at the Fermi level. The mechanical deformation of some Pt nanotubes can induce a formation minigaps in a terahertz region that can be used in electronic devices.

1. Introduction

The noble metal nanotubes are of great interest in the mesoscopic physics, chemistry, and catalysis and they are very promising for use in nanotechnology such as in a fabrication of electronic devices. Various techniques [1–7] are developed to synthesize the Pt, Au, Pd, and Ag nanotubes and they are focus of many interdisciplinary studies. Particularly, the single-walled platinum nanotubes can be obtained starting from platinum nanowire and applying an electron-beam thinning method. Such nanotubes have the triangular network with atom rows helically coiling around the wire axis [1,2]. The helical metal nanotubes have been intensively investigated theoretically and experimentally and it is reported that the nanotubes have distinct electronic and mechanical properties, quantum ballistic transport, and conduction channels originating from their helical structure [8–14]. However, to best of our knowledge, there has been no detailed study of a band structure of the platinum nanotubes, which are expected to have the electron properties quite different from those of the Pt bulk or surfaces [15–18], because the Pt atoms in nanotube have two times smaller coordination number and the electron properties of nanotubes are to be sensitive to their chirality and diameter. The calculations of Pt nanotubes are limited to works [19–22]. In paper [20], in the terms of a projected augmented wave method and density functional theory, the dispersion curves of achiral (6, 6) and (13, 13) Pt nanotubes for the Fermi energy region were calculated. In work [19], the structures, magnetic moments, and densities of states (DOS) of finite length Pt nanotubes were calculated using similar approach and plane-wave basis set. Finally, some data on the DOS of Pt (6, 4) and (5, 3) nanotube were obtained using the supercell cluster calculations and plane wave basis [22]. However, in the calculations [19–22], the spin-orbit coupling terms were not taken into account in Hamiltonian, but the spin-orbit term must gives rise to a splitting of energy bands and formation of spin-obit gaps. Platinum is a heavy metal; for its compounds, the spin-orbit interaction should be surely taken into consideration. Moreover, in the case of nanotubes, the spin-orbit interaction manifests itself particularly strongly; due to the nanotubes cylindrical structure, the electron states correspond to the semiclassical clockwise and anticlockwise electron orbits encircling the tubule and resulting in the large values of orbital magnetic moment and

* Corresponding author.
E-mail address: p_dyachkov@rambler.ru (P.N. D'yachkov).

https://doi.org/10.1016/j.cplett.2019.02.006
Received 13 December 2018; Received in revised form 31 January 2019; Accepted 1 February 2019
Available online 13 February 2019
0009-2614/

spin-orbit coupling even in the case of carbon tubules [23–25]. Thus, a calculation of the spin-dependent band structure of Pt nanotubes is an actual problem.

The nanotubes may be subjected to various mechanical deformations such as twisting, stretching, contraction, bending, or flattening, and physical properties of tubules can be tuned by controlling their shape [26–33]. This area of research, called nanoelectromechanics, demonstrates a rapid development and is crucial to the nanotubes optical and electronic properties understanding and applications. The electromechanical properties of carbon nanotubes were first studied. The dispersion relations and DOS of deformed carbon nanotubes with different chiralities and deformation modes were analyzed theoretically based on the Hückel tight-binding model [34] and their electromechanical responses have been observed for axial [28,29], radial [30], flexural [31], and torsional [35] strains, many types of devices such as strain, motion, atomic-scale mass sensors, nanoscopic pendulums, nanoactuators, nanoaccelerometers, nanobalances, and nanogyroscopes being envisioned and realized [33,36–39]. Latter, the deformation-driven electron transport and piezoelectricity were studied for individual BN nanotubes [40,41]; the features of mechanics and electromechanics of BCN tubules were analyzed and ultrahigh torsional stiffness was detected suitable for application in the highly sensitive electromechanical transducers [42]; the theoretical and experimental study of the electromechanical behavior of WS_2 nanotubes shows that material exhibits a complex and reproducible electrical response to mechanical deformations and that it is applicable for design of highly sensitive nanometric motion sensors and resonators [43,44]. The effect of mechanical deformation on the electronic properties of the Pt nanotubes has not been previously studied.

It is the aim of this work to study the spin- and deformation-dependent electron structures of the single-walled Pt nanotubes. For this purpose, we calculate the band structures and DOS of chiral and achiral Pt tubules in terms of a relativistic symmetrized linear augmented cylindrical wave (LACW) method [45–47] and use the results to predict their electron and electromechanical properties.

2. Method of calculation

The LACW method described in detail elsewhere [45–47] is just a reformulation of the relativistic linear augmented plane wave (LAPW) theory for tubular multiatomic systems. The calculations are based on the two-component relativistic Hamiltonian

$$H = -\Delta + V(\mathbf{r}) + \frac{1}{c^2}\boldsymbol{\sigma}\cdot[(\nabla V)\times\mathbf{p}] \tag{1}$$

Here, $-\Delta + V(\boldsymbol{r})$ is a nonrelativistic part of the operator and the third term is a spin-orbit coupling. The atomic units are used, c is speed of light and $\boldsymbol{\sigma}$ is the Pauli matrix. For electron potential $V(\boldsymbol{r})$, the approximations are made in the sense of muffin-tin potentials and local density functional theory only. In this model, the electronic band structure of a nanotube is determined by the free electron movement in the cylindrical interspherical region and by electron scattering on the muffin-tin potentials. The method applied here takes into account the screw and rotational symmetries of nanotubes and is applicable to any platinum tubule independent on diameter and chirality. The structural information is used as input parameters.

Structure of any Pt nanotube can be generated by first mapping one atom onto the surface of a cylinder and then using the rotational C_n and helical $S(h,\omega)$ symmetry operators to determine the remainder of the tubule. The nanotubes are characterized with two indices (n_1,n_2). The cylinder axis coincides with the C_n rotational axis for the tubule, where n is the largest common divisor of n_1 and n_2. The helical motif of the tubule is determined by repeated operation of a translation

$$h = \frac{n\sqrt{3}\,d}{2(n_1^2 + n_2^2 + n_1 n_2)^{1/2}} \tag{2}$$

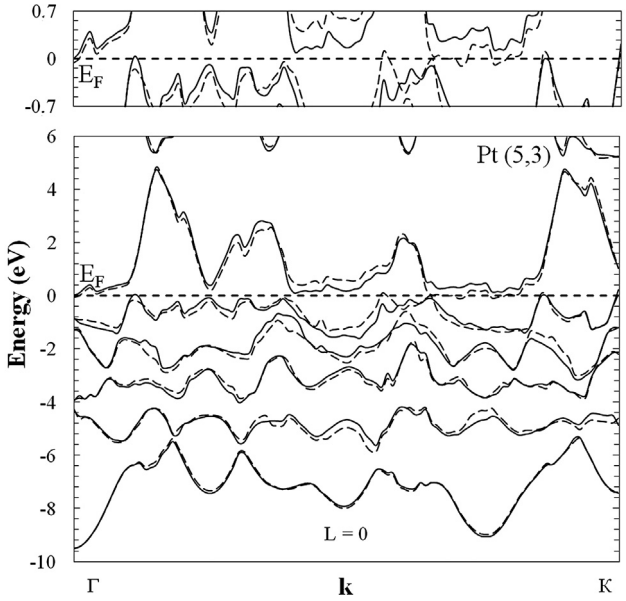

Fig. 1. Band structure of the (5, 3) Pt nanotube. The dashed and solid lines correspond to the band states with spin α and β spins, respectively. The dispersion curves in the Fermi energy region are presented in enlarged energy scale.

along the cylinder axis in conjunction with a rotation

$$\omega = 2\pi\frac{p_1 n_1 + p_2 n_2 + (p_2 n_1 + p_1 n_2)/2}{n_1^2 + n_2^2 + n_1 n_2} \tag{3}$$

rad about this axis. Here, $d = 2.82$ is Pt—Pt bond length and the positive integers p_1 and p_2 are obtained from the equation $p_2 n_1 - p_1 n_2 = n$. The eigenstates depend on the two quantum numbers, namely, the rotational quantum number $L = 0, 1, \ldots, n-1$ and the wave vector $0 \le k \le \pi/h$ corresponding the screw translations.

3. Results and discussion

Fig. 1 shows the results of calculations of the band structure of tubule (5, 3). This is the chiral system without rotational symmetry having 98 atoms per translational unit cell. However, due to account of screw symmetry, the cell is reduced to one atom and the results are presented in a very simple form with only ten spin-dependent energy bands in the valence band and two low-energy curves in the conduction band. The Fermi level clearly separates the valence and conduction band curves. There is no crossing of the occupied and vacant dispersion curves, but only slight overlap of a top of valence and of a bottom of conduction states typical for semimetallic systems. In the band structure, the spin-orbit coupling appears as the large splitting of nonrelativistic dispersion curves equal up to 0.5 eV for the bands in Fermi energy region. The spin-polarization of eigenstates relative to the nanotube axis is almost perfect (> 99%), the polarization directions being opposite for split pairs of bands.

Band structure is presented for positive values of the wave vectors k only, because in the case of chiral tubule the dispersion curves are antisymmetric with respect to substitution k for –k; due to Kramers theorem, they have the same energies, but opposite polarization of spins.

$$E(\mathrm{k},\alpha) = E(-\mathrm{k},\beta) \tag{4}$$

Moreover, as usual for molecules with helical symmetry, in the case of Pt (5, 3) nanotube the pairs of E(k,α) and E(–k,β) states with the same energies but opposite spins are characterized by the opposite electron velocities.

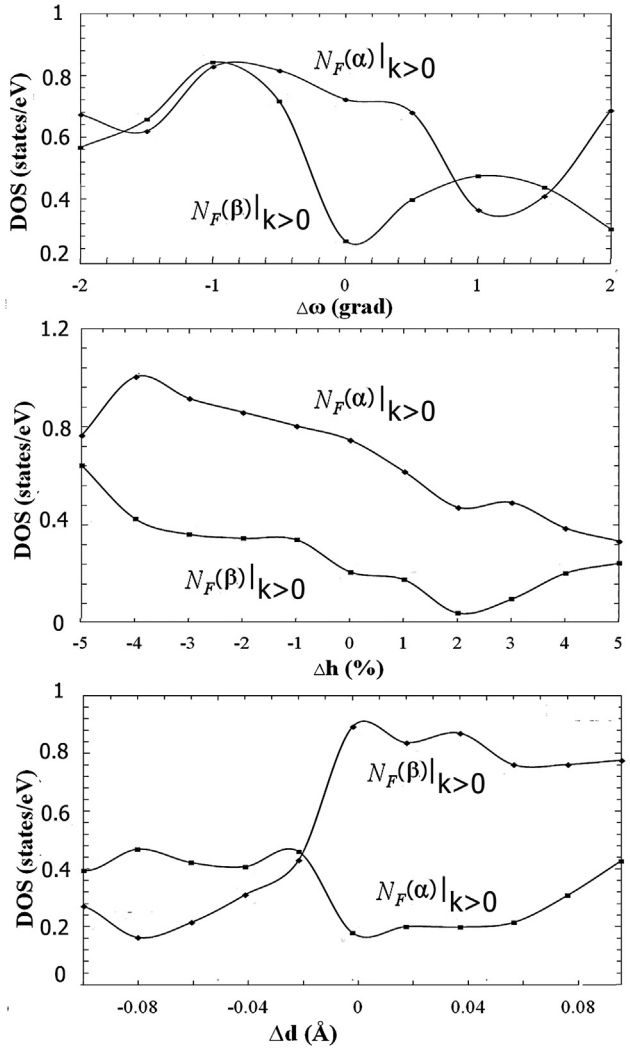

Fig. 2. Change of electron DOS $N_F(\alpha)|_{k>0}$ and $N_F(\beta)|_{k>0}$ on the Fermi level in the cases of torsional Δω and uniaxial strains, and for Pt—Pt bond variations of chiral (5, 3) Pt nanotube. Here, $\Delta\omega > 0$ for chirality increase and $\Delta\omega < 0$ for decrease; $\Delta h > 0$ for tension and $\Delta h < 0$ for compression; $\Delta d > 0$ for stretching and $\Delta d < 0$ for shortening.

$$dE(k, \alpha)/dk = -dE(-k, \beta)/dk \quad (5)$$

Recent theoretical and experimental studies have shown that the electron transport through molecules with helical geometry can be spin-dependent, the preferred spin-orientation being determined by the chirality of molecule and by direction of electron motion [48–50]. The effect is known as chirality-induced spin selectivity. Fig. 2 shows the calculated spin-dependent DOS on the Fermi level for the electrons with spin up $N_F(\alpha)|_{k>0}$ and spin down $N_F(\beta)|_{k>0}$ for the Brillouin zone $k > 0$. For unstressed Pt (5,3) tube, the $N_F(\alpha)|_{k>0}$ is about three times larger than the $N_F(\beta)|_{k>0}$, and so the concentration of mobile electrons with spin α is three times greater than with spin β for the electron movement along the tube axis in positive direction. The Eqs. (4) and (5) show that for $k < 0$ the situation is reversed, the $N_F(\beta)|_{k<0} \approx 3\, N_F(\alpha)|_{k<0}$ and transport of electrons with β spin will dominate in the opposite direction.

In the case of the (5,3) Pt nanotube, the DOS of mobile electrons $N_F(\alpha)|_{k>0}$ and $N_F(\beta)|_{k<0}$ with different spins can be tuned by torsional, uniaxial, and uniform strains. Fig. 2 shows the variations of the $N_F(\alpha)|_{k>0}$ and $N_F(\beta)|_{k>0}$ due to the nanotube torsional and uniaxial strains described in the terms of Δω and Δh parameters as well as due to the Pt—Pt bonds change Δd. The torsion of the (5, 3) nanotube with

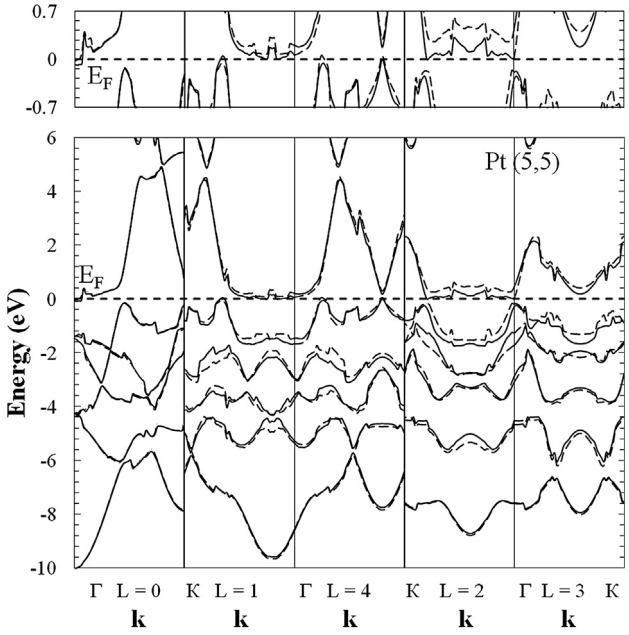

Fig. 3. Band structure and DOS of the (5, 5) Pt nanotube.

positive and negative values of the Δω corresponds to the chirality increase and decrease. The change of ω by about ± 1 grad results in a rapid increase of the $N_F(\beta)|_{k<0}$ and leveling of the concentration of mobile α and β electrons. The twisting of the nanotube (5, 3) with $\Delta\omega = \pm 2$ grad makes it possible to double the total DOS $N_F = N_F(\alpha) + N_F(\beta)$ at the Fermi level. Uniaxial compression of the nanotube (5, 3) within 5% leads to an increase of $N_F(\alpha)$ and $N_F(\beta)$, but analogous stretching, to the descending of the $N_F(\alpha)$ and $N_F(\beta)$. In the strain range studied, the inequality $N_F(\alpha)|_{k>0} > N_F(\beta)|_{k>0}$ is satisfied. The uniaxial compression and stretching of the nanotube (5, 3) within $\Delta h = \pm 5\%$ lead to the oscillatory increase and decrease of the N_F. The uniform compression of the nanotube with $|\Delta d| < 0.1$ Å causes a rapid decrease in $N_F(\alpha)|_{k>0}$ and increase in $N_F(\beta)|_{k>0}$, the concentrations of mobile α and β electrons become equal at the $\Delta d = -0.02$ Å. The uniform compression and extension of the nanotube with a change in d causes the decrease and increase in N_F, respectively.

Fig. 3 shows the band structure of the (5, 5) nanotube, which is characterized by the 5th order rotational axes in addition to the screw translations. In the repeated zone scheme, there are three sets of dispersion curves: for the rotational quantum numbers $5 - L$, the bands are continuous extensions of the bands for L. Again, the curves for valence and conduction states are separated and the tubule is semimetallic with significant spin-orbit splitting. Due to inversion symmetry of this tubule, the electron transport does not dependent on the spins of mobile electrons.

The uniaxial compression is accompanied by small variations of the N_F, but the uniaxial extension results in a rapid decrease of the N_F, and the optical gap opens at $\Delta h \geq 3\%$ and rises up to $E_g = 50$ meV at $\Delta h = 5\%$ (Fig. 4). The decrease of N_F is the result of small positive and negative changes of the Pt-Pt bond length, and the optical gap up to 50 meV opens between the valence and conduction bands at $\Delta d \leq -0.15$ Å. The torsions ± Δω turn the achiral tubule into chiral one, the effect being independent on direction of torsion. The DOS N_F is the decreasing function of Δω for $0 < \Delta\omega < 1$ grad, but N_F increases for Δω between 1 and 2 grads. The chirality-induced spin selectivity is negligible for these small torsions of the (5, 5) nanotube.

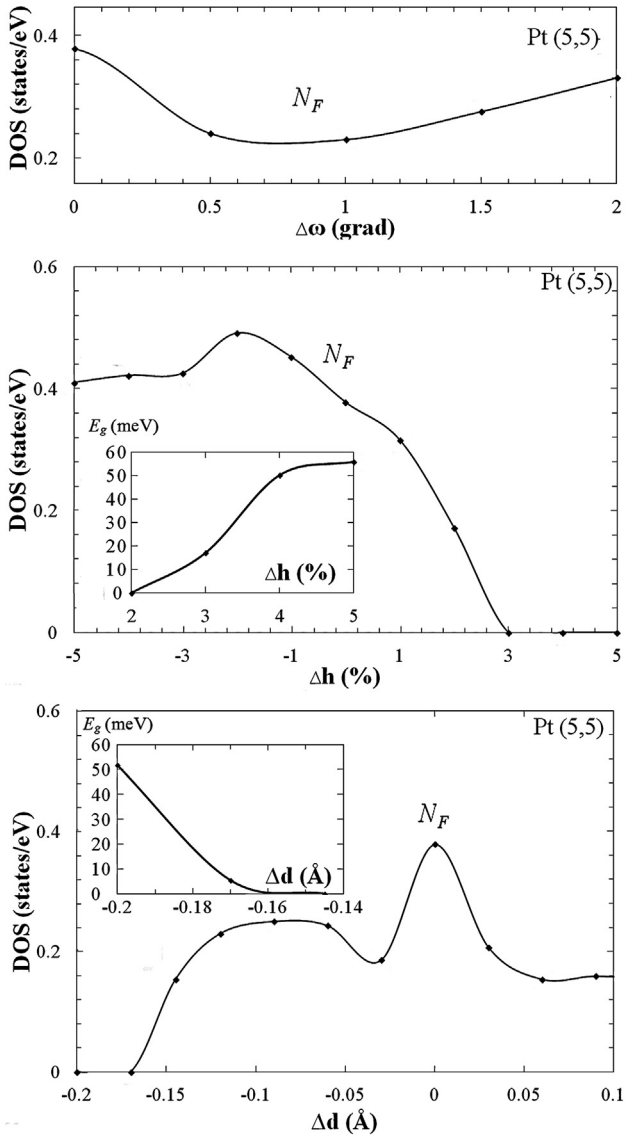

Fig. 4. Effects of deformation of (5, 5) Pt nanotube on the Fermi level DOS N_F.

4. Conclusion and discussion

Thus, the relativistic LACW results show that single-walled Pt nanotubes are the semimetallic compounds with Fermi level separating the valence and conduction band curves and with spin-orbit splitting of band states equal up to 0.5 eV. The spin-dependent electron transport can be controlled by mechanical deformation of the chiral Pt tubules. In some Pt nanotubes, the optical gap can be open in the terahertz region and used in terahertz electronic devices. Note that the LACW bands reasonably correlate with available nonrelativistic calculations of Pt nanotubes. The gaps equal to 0.02–0.15 eV that are smaller than the expected spin-orbit splitting open in the small Pt tube clusters[19], and $E_g = 0$ in the infinite single-walled [19] and double-walled [22] Pt nanotubes. In a reasonable agreement with our data on the spin-orbit coupling effects in the Pt nanotubes, the spin-orbit splitting of different bands in the Brillouin zone high-symmetry points of the fcc bulk platinum are equal to the 0.35–1.09 eV according to the relativistic LAPW method [15,16]. The valence band widths of the Pt nanotubes $E_v = 10$ eV are virtually the same as in the fcc bulk platinum and in the platinum low–index surfaces calculated using the relativistic and full-potential LAPW technique [15,16,18].

Declaration of interests

The author declares that there is no conflict of interest.

References

[1] Y. Oshima, H. Koizumi, K. Mouri, et al., Phys. Rev. B 65 (12) (2002) 121401(R).
[2] Y. Oshima, A. Onga, K. Takayanagi, Phys. Rev. Lett. 91 (20) (2003) 205503.
[3] Z. Huang, D. Raciti, S. Yu, et al., J. Am. Chem. Soc. 138 (20) (2016) 6332–6335.
[4] Y. Bi, G. Lu, Electrochem. Commun. 11 (1) (2009) 45–49.
[5] X.W. Lou, L.A. Archer, Z. Yang, Adv. Mater. 20 (21) (2008) 3987–4019.
[6] G. Zhang, S. Sun, M. Cai, et al., Scient. Rep. 3 (2013) 1526.
[7] W.R. Hendren, A. Murphy, P. Evans, et al., J. Phys.: Condens. Matter 20 (36) (2008) 362203.
[8] Y. Oshima, K. Mouri, H. Hirayama, K. Takayanagi, J. Phys. Soc. Jpn. 75 (5) (2006) 053705.
[9] M. del Valle, C. Tejedor, G. Cuniberti, Phys. Rev. B 74 (4) (2006) 045408.
[10] A. Sen, C.J. Lin, C.C. Kaun, J. Phys. Chem. C 117 (26) (2013) 13676–13680.
[11] T. Ono, K. Hirose, Phys. Rev. Lett. 94 (20) (2005) 206806.
[12] K. Zhang, H. Zhang, J. Phys. Chem. C 118 (1) (2014) 635–641.
[13] T. Shimada, Y. Ishii, T. Kitamura, Phys. Rev. B 84 (16) (2011) 165452.
[14] D. Zs, J. Cserti Manrique, C.J. Lambert, Phys. Rev. B 81 (7) (2010) 073103.
[15] O.K. Andersen, Phys. Rev. B 2 (4) (1970) 883–907.
[16] A.K. Bordoloit, S. Auluck, J. Phys. F: Met. Phys. 13 (10) (1983) 2101–2105.
[17] H. Wern, R. Courths, G. Leschik, S. Hüfner, Phys. B Condens. Matter 60 (2–4) (1985) 293–310.
[18] H.J. Herrera-Suárez, A. Rubio-Ponce, D. Olguín, Revista Mexicana de Física 58 (1) (2012) 46–54.
[19] L. Xiao, L. Wang, Chem. Phys. Lett. 430 (4–6) (2006) 319–322.
[20] I. Matanović, P.R.C. Kent, F.H. Garzon, N.J. Henson, J. Electrochem. Soc. 160 (6) (2013) F548–F553.
[21] L. Hui, F. Pederiva, W. Guanghou, W. Baolin, Chem. Phys. Lett. 381 (1–2) (2003) 94–101.
[22] S. Konar, B.C. Gupta, Phys. Rev. B 78 (23) (2008) 235414.
[23] T. Ando, J. Phys. Soc. Jpn. 69 (6) (2000) 1757–1763.
[24] E.D. Minot, Y. Yaish, V. Sazonova, P.L. McEuen, Nature 428 (6982) (2004) 536–539.
[25] F. Kuemmeth, S. Ilani, D.C. Ralph, P.L. McEuen, Nature 452 (7186) (2008) 448–452.
[26] H.G. Craighead, Science 290 (5496) (2000) 1532–1535.
[27] A. Maiti, Nat. Mater. 2 (7) (2003) 440–442.
[28] T.W. Tombler, C. Zhou, L. Alexseyev, et al., Nature 405 (6788) (2000) 769–772.
[29] E.D. Minot, Y. Yaish, V. Sazonova, et al., Phys. Rev. Lett. 90 (15) (2003) 156401.
[30] C. Gómez-Navarro, P.J. de Pablo, J. Gómez-Herrero, Adv. Mater. 16 (6) (2004) 549–552.
[31] V. Semet, V.T. Binh, D. Guillot, et al., Appl. Phys. Lett. 87 (22) (2005) 223103.
[32] V. Sazonova, Y. Yaish, H. Üstünel, et al., Nature 431 (7006) (2004) 284–287.
[33] E. Joselevich, ChemPhysChem 7 (7) (2006) 1405–1407.
[34] L. Yang, J. Han, Phys. Rev. Lett. 85 (1) (2000) 154–157.
[35] T. Cohen-Karni, L. Segev, O. Srur-Lavi, et al., Nat. Nanotechnol. 1 (1) (2006) 36–42.
[36] H.Y. Chiu, P. Hung, H.W.C. Postma, M. Bockrath, Nano Lett. 8 (12) (2008) 4342–4346.
[37] K. Jensen, K. Kim, A. Zettl, Nat. Nanotechnol. 3 (9) (2008) 533–537.
[38] B. Lassagne, D. Garcia-Sanchez, A. Aguasca, A. Bachtold, Nano Lett. 8 (11) (2008) 3735–3738.
[39] J.C. Meyer, M. Paillet, S. Roth, Science 309 (5740) (2005) 1539–1540.
[40] Y.H. Kim, K.J. Chang, S.G. Louie, Phys. Rev. B 63 (20) (2001) 205408.
[41] X. Bai, D. Golberg, Y. Bando, et al., Nano Lett. 7 (3) (2007) 632–637.
[42] J. Garel, C. Zhao, R. Popovitz-Biro, et al., Nano Lett. 14 (11) (2014) 6132–6137.
[43] R. Levi, J. Garel, D. Teich, et al., ACS Nano 9 (12) (2015) 12224–12232.
[44] Y. Divon, R. Levi, J. Garel, et al., Nano Lett. 17 (1) (2016) 28–35.
[45] P.N. D'yachkov, D.V. Makaev, Phys. Rev. B 76 (19) (2007) 195411.
[46] P.N. D'yachkov, D.Z. Kutlubaev, D.V. Makaev, Phys. Rev. B 82 (3) (2010) 035426.
[47] P.N. D'yachkov, D.V. Makaev, Intern. J. Quant. Chem. 116 (4) (2016) 316–324.
[48] K. Banerjee-Ghosh, O.B. Dor, F. Tassinari, et al., Science 360 (6395) (2018) 1331–1334.
[49] R. Naaman, D.H. Waldeck, Annu. Rev. Phys. Chem. 66 (2015) 263–281.
[50] R. Gutierrez, E. Díaz, C. Gaul, T. Brumme, et al., J. Phys. Chem. C 117 (2013) 22276–22284.